

## **STYLIZED VERSUS TOMOGRAPHIC: AN EXPERIENCE ON ANATOMICAL MODELING AT RPI**

**X. George Xu**

Nuclear Engineering and Engineering Physics Program  
Rensselaer Polytechnic Institute  
Troy, NY 12180, USA  
xug2@rpi.edu

### **ABSTRACT**

This invited paper summarizes our experience in using both the MIRD-type stylized models and tomographic models at Rensselaer. Comparisons are made of the scaled-down version of the tomographic VIP-Man model with the stylized adult male model for external photon beams. Similar comparisons are made to a stylized pregnant woman model and a tomographic model for internal photons. The effective dose results from these two models show that they differ from each other within about 10% for common high-energy photon beams, and the SAFs for the pregnant woman for photon energies above 50 keV are very similar between the two types of model. It is concluded that the use of tomographic models may not improve the operational radiation protection dosimetry involving photon exposures due to the large uncertainty already existed in the radiation protection quantities. It is also noted that the voxelized models have some major disadvantages and the radiation protection dosimetry community should consider hybrid approaches involving image-based voxels and advanced surface equations in the future.

*Key words:* Stylized Model, Tomographic Model, Effective Dose, Monte Carlo.

### **1 INTRODUCTION**

Doses at the organ level are necessary in three different applications: radiation protection, radiation epidemiology, and radiotherapy. These three applications require different approaches and are expected to contain different degrees of uncertainty. Due to the large uncertainty in radiation and tissue weighting factors, one might tolerate up to 50% uncertainty in the derived radiation protection quantities. On the other hand, a treatment plan for external radiation beam requires the uncertainty in the calculated doses to be less than a few percent. Epidemiological dosimetry also needs to be very accurate because the derived dose response function is fundamentally important in risk assessment. One major contribution to the uncertainty in an assessed organ dose is the anatomical geometry used in Monte Carlo calculations to define a worker (or patient). To date, two types of anatomical models have been developed: 1) Equation-based stylized models, where organs are delineated by a combination of simple surface equations, and 2) Image-based tomographic models, in which organs are defined from segmented

and labeled volume elements (voxels) from tomographic images of real individuals. A third and emerging type of models may be defined as a hybrid of these two.

For almost three decades, the *de facto* standard for human models used for radiation protection dosimetry had been the so-called MIRD-type stylized mathematical models originally developed since the 1970s at Oak Ridge National Laboratory for the Medical Internal Radiation Dose (MIRD) Committee of The Society of Nuclear Medicine [1,2]. In the past 15 years, however, the radiation protection dosimetry community has gradually favored a new class of human models called tomographic (or voxel) models that are based on segmented medical images. To date, more than 20 such tomographic models have been constructed [3]. In an ICRP Annual Report in 2002, a paradigm shift in radiation protection dosimetry was officially recognized: “ An important issue for Committee 2 is the substitution of an anatomically realistic voxel phantom, obtained digitally in magnetic resonance tomography and/or computed tomography, for the MIRD phantom which is a mathematical representation of a human body ” [4]. The ICRP has further recommended the uses of tomographic models in its 2005 recommendations [5]. Past recommendations from ICRP have been eventually adopted by agencies in the United States, including NRC, NCRP, EPA, and FDA, thus affecting every aspects of protection against ionizing radiation.

The hypothesis driving the development of tomographic models was that a greater realism in the models would improve the radiation protection dosimetry. Our work at Rensselaer in this aspect involved both stylized and tomographic models. In particular, we recently produced two tomographic models: one adult male called VIP-Man [6-10] and one model for a pregnant woman [11,12]. This paper examines the advantages and disadvantages of these two types of the models in terms of anatomical representation, implementation in Monte Carlo codes, and the changes in the derived organ doses.

## 2. MATERIALS AND METHODS

### 2.1 Stylized models

Stylized anatomical models were originally developed for the Medical Internal Radiation Dosimetry (MIRD) Committee of the Society of Nuclear Medicine (SNM) in 1970's [1,2]. Later improvement at Oak Ridge led to the development of a “family” of models [13]. This type of models has been called by various names such as MIRD, ORNL, mathematical or Cristy-Eckerman models. Since MIRD is now adopting other types of models, we may want to just use the term “MIRD-stylized models.” The original MIRD stylized adult male model was developed to mimic the “Reference Man” defined by ICRP for radiation protection purposes [14]. More than 40 organs and tissues were specified, with basically three media of distinct densities: bone, soft tissue, and lung. These models were analytically defined in three principal sections: an elliptical cylinder representing the arm, torso, and hips; a truncated elliptical cone representing the legs and feet; and an elliptical cylinder representing the head and neck..

Fig. 1a shows the skeleton and internal organs of the adult male. Fig. 1b details the stomach and gastrointestinal (GI) tract. The series of “family” stylized models are summarized in Fig.

1c, including both genders at ages of 15 (also the female adult), 10, 5, 1, and 0 (new born) [13]. Using similar approaches, models of fetal and pregnant woman have been developed [15]. Fig. 1d shows a 9-month pregnant woman.

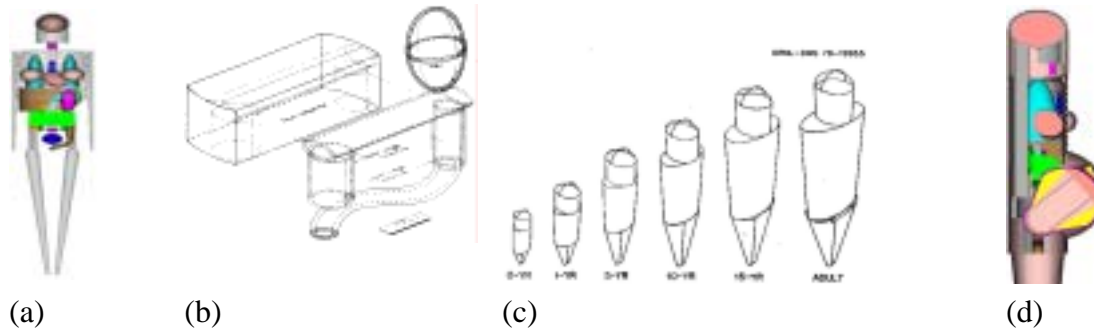


**Figure 1.** Stylized models showing (a) exterior view of the adult male, (b) surface equations representing stomach and GI tract of the adult male, (c) “family” of both genders of different ages. (d) The 9-month pregnant woman.

The stylized mathematical descriptions of the organs were formulated based on descriptive and schematic materials from general anatomy references. The goal of this approach was to make the equations simple, thus minimizing computing time. For example, the stomach wall (the football shape in Fig. 1c) is defined as the volume between two concentric ellipsoids [13]:

$$\left(\frac{x-x_0}{a}\right)^2 + \left(\frac{y-y_0}{b}\right)^2 + \left(\frac{z-z_0}{c}\right)^2 \leq 1 \quad \text{and} \quad \left(\frac{x-x_0}{a-d}\right)^2 + \left(\frac{y-y_0}{b-d}\right)^2 + \left(\frac{z-z_0}{c-d}\right)^2 \geq 1. \quad (1)$$

These surface equations are compatible with the geometry definitions in most Monte Carlo radiation transport codes, making the organ dose calculations possible since 1970s. For thirty years, these virtual models have made important contributions to studies in radiation protection, nuclear medicine, and medical imaging. Although the ICRP has never officially endorsed these stylized models, it has recommended a large amount of fluence-to-dose-equivalent conversion coefficients that were calculated from these stylized models [16,17]. The shortcomings of these models became obvious in late 1980’s. Human anatomy was too complex to be truthfully modeled with a limited set of equations. As such, many anatomical details in the stylized models had to be compromised and the geometry remains simplified and crude. For instance, the skeleton in the model does not resemble a human.

## 2.2. Tomographic Models

In the past 15 years, a new class of computational models has emerged with the advent of 3D tomographic imaging. These models contain large arrays of voxels that are identified in terms of tissue type (soft tissue, hard bone, air, etc) and unique organ identification (lungs, liver, skin, etc). Tomographic images reveal patient internal structures accurately, but time-consuming segmentation and classification are necessary to implement the models for radiation transport calculations in a Monte Carlo code. To date, a number of major studies have reported

whole-body tomographic models constructed with this approach by researchers from Germany, UK, Korea, Japan, Australia, Brazil and U.S. [3].

In 1997, Rensselaer started to develop an adult male patient model, called VIP-Man [6]. This model was based on anatomical color images of the Visible Man from the Visible Human Project (VHP) [18] as shown in Fig. 2. The subject whose images were used to develop the VIP-Man model was 186-cm tall and 90 kg in weight. Major organs in the original VIP-Man model have similar masses than the Reference Man, however, the total body height and weight were not [26]. The body had an increase in body volume after it was frozen, causing the weight also to increase to 104 kg because the tissue densities were assumed to be unchanged in the calculations. More than 1400 organs and tissues were segmented, among which about 70 radio-sensitive ones were adopted for Monte Carlo calculations. VIP-Man model has been successfully used for Monte Carlo radiation studies of organ doses for photons [7-10], as well as for electrons, neutrons and protons. Papers on the VIP-Man model can be downloaded from the web site of the Rensselaer Radiation Measurements and Dosimetry Group (RRMDG.rpi.edu). A scaled-down version of VIP-Man at 176-cm tall and 73 kg in weight was developed by universally reducing the voxel dimensions of the original VIP-Man model. For photon and electron calculation in EGS4 code [7-10], the voxel size was reduced from 0.33mm x 0.33mm x 1.0 mm to 0.286mm x 0.286 mm x 0.946 mm. VIP-Man model has been shared with interested researchers for free, and please contact the author for more information.

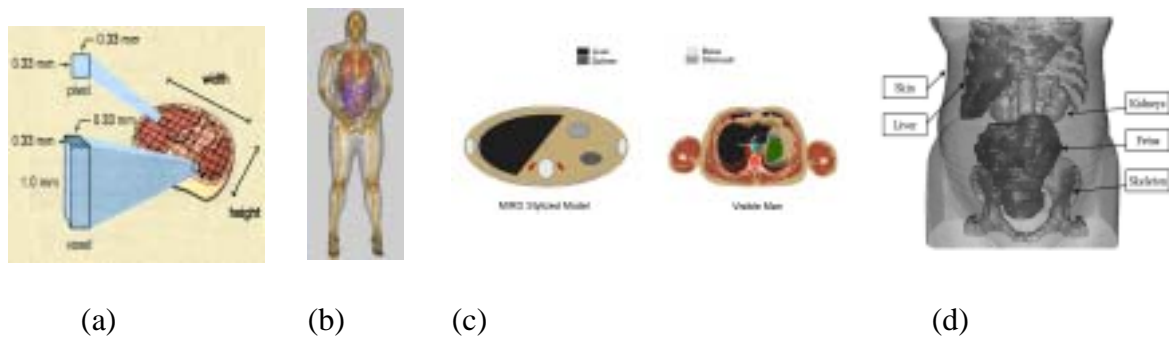


**Figure 2.** (a) 3D voxels geometry; (b) 3D rendering of the VIP-Man model; (c) Slices showing anatomical difference between the two types of models. (d) A tomographic model of 7-month pregnant woman.

Also developed at Rensselaer was a partial-body pregnant woman model from segmented CT images [11, 12]. The CT image data of a pregnant patient was collected from a hospital where the patient was scanned during a life-saving procedure. The 31 years old patient was 30 weeks pregnant and her weight was 91 kg. The scans covered the portion of her body between lower breast and thigh. A total of 70 slices were finally selected to construct the tomographic model, with each slice being 7 mm thick. The view size of the image is 480 mm×480 mm with 512×512 pixels; therefore, the image resolution is 0.94 mm/pixel and 3D voxel size is 0.94 mm×0.94 mm×7 mm. The 3D rendering of the model with organs labeled is shown in Fig. 2d.

## 2.3 Dose Calculation Procedures

Dose calculation algorithms were based on ICRP 60 [19]. The mean absorbed dose in an organ or tissue ( $D_T$ ) was calculated as the total energy deposited in organ T per unit mass. The equivalent dose ( $H_T$ ) in T was calculated by multiplying the mean absorbed dose by the radiation weighting factor,  $w_R$ . Tissue weighting factors ( $w_T$ ) were finally used to calculate ED using Equation 1,

$$E = \sum_T w_T H_T \quad (\text{Eq. 1})$$

Twelve critical organs/tissues and their weighting factors explicitly recommended by ICRP 60 [19]. The bone surface, which is in the scale of  $\sim 10 \mu\text{m}$ , was too small to be defined in VIP-Man. Consequently, the dose to bone surface was substituted with the dose to bone. The only available testis in VIP-Man was used to represent gonads and a thin layer of fat tissue around chest level was used for each breast. Ten more organs and tissues are included in the “remainder” organ which share a total tissue weighting factor of 0.05. The upper large intestine was later combined to the critical organ, colon. Thus, the VIP-Man model has only eight remainders (there is no uterus in the VIP-Man model). In accordance with ICRP recommendations, if one of the “remainder” organs receives the highest equivalent dose of the twelve specified organs, a weighting factor of 0.025 was applied to this organ, and the other 7 remainders would share the remaining 0.025. Otherwise, all eight remainders shared the 0.05.

## 2.4 Implementation of the tomographic models in Monte Carlo Codes

The scaled VIP-Man anatomical definition contains a total of about 3.7 billion voxels, each having a size of 0.286mm x 0.286 mm x 0.946 mm. This huge amount of data had to be compressed and coded using the EGS4-VLSI (Very Large Segmented Images) user code for photon and electron calculations [7-10]. The scaled VIP-Man model was implemented in EGS4-VLSI code in dual CPU machines with a typical 512-MB RAM under Linux operating system. Radiation sources considered in this study were monoenergetic parallel beams of photons with energies range from 10 keV to 10 MeV. The irradiation geometries include antero-posterior (AP), postero-anterior (PA), left lateral (LLAT), right lateral (RLAT), rotational (ROT), and isotropic (ISO). The model is irradiated in vacuum. The pregnant woman model was also implemented in the EGS4-VLSI code in a similar manner [11-12]. Internal photon sources are simulated in the pregnant woman model to calculate specific absorbed fractions (SAFs). For implementation in MCNP and GEANT4 codes, please visit RRMDG.rpi.edu.

# 3 RESULTS

## 3.1 Anatomy

We first compare organ masses of various models and recommended data. Table 1 lists the organ masses of the original VIP-Man model, the scaled VIP-Man model, the Reference Man [14] and the MIRD stylized adult male model [13] all using very similar densities. As expected, the discrepancies between models are found for all organs. It is noted that the scaled-down VIP-Man model is fatty, which means that most organs weigh less than the stylized model and

the Reference Man in order for the total body weight to agree. The lungs in the VIP-Man model are considerably smaller because of the supine position that compressed the organ. Similarly, the organ masses for the pregnant woman model are compared with the stylized model and the Reference Woman in Table II.

Table I. Comparison of organ masses for VIP-Man, MIRD Mathematical Phantom, and ICRP Reference Man.

Organs/tissues	VIP-Man (g)	Scaled VIP-Man (g)	MIRD (g)	Reference Man (g)
Adrenals	8.3	5.8	16.3	14.0
Bladder (wall)	41.4	29.0	47.6	45.0
Bladder (urine)	43.2	30.2	211.0	102.0
Brain + Nerve	1,574.0	1,101.9	1,420.0	1,429.0
Breast (male)	33.6	23.5	403.0	26.0
CSF	265.1	185.6	--	121.0
Esophagus (wall)	38.9	27.2	--	40.0
Esophagus (lumen)	26.8	18.8	--	--
Esophagus (mucosa)	3.5	2.5	--	--
Fat	36,326.6	25,430.7	--	17,200.0
Gall bladder (wall)	12.0	8.4	10.5	10.0
Gall bladder (bile)	21.0	14.7	55.7	60.0
Heart muscle	398.7	279.1	316.0	330.0
Kidneys	335.4	234.8	299.0	310.0
Lens of eyes	0.54	0.4	--	0.4
Liver	1,937.9	1,356.6	1,910.0	1,800.0
Lower Large intestine (wall)	290.8	203.6	167.0	160.0
Lower Large intestine (lumen)	324.2	227.0	143.0	135.0
Lower Large intestine (mucosa)	35.8	25.1	--	--
Lungs	910.5	637.4	1,000.0	1,000.0
Muscle	43,002.6	30,104.3	--	28,000.0
Pancreas	82.9	58.0	94.3	100.0
Prostate	18.9	13.2	--	16.0
Red Bone Marrow	1130.4	791.2	--	1,500.0
Skeleton	10114.2	7,080.7	10,000.0	8,500.0
Skin	2,253.4	1,577.5	3,010.0	2,600.0
Small intestine	1,291.8	904.3	1,100.0	1,040.0
Spleen	244.0	170.8	183.0	180.0
Stomach (wall)	159.5	111.7	158.0	150.0
Stomach (content)	324.5	227.2	260.0	250.0
Stomach (mucosa)	13.7	9.6	--	--

Testes	21 (1)	14.7	39.1	35.0
Thymus	11.2	7.8	20.9	20.0
Thyroid	27.6	19.3	20.7	20.0
Upper Large intestine (wall)	461.1	322.8	220.0	160.0
Upper Large intestine (lumen)	905.7	634.0	232.0	135.0
Upper Large intestine (mucosa)	63.4	44.4	--	--
Other	1,688.0	1,181.7	51,887.7	4,382.0
Total	104,277.2	73,000.0	73,224.8	73,000.0

**Table II. Comparison of organ mass of the pregnant woman with different models.**

<b>Organs</b>	<b>CT pregnant woman Mass (g)</b>	<b>Mathematical model <sup>a</sup> Mass (g)</b>	<b>Reference Woman Mass (g)</b>
Adrenals	14.10	14	14
Fetus	1715.72	1640	(1250--1750) <sup>c</sup>
Soft tissue of fetus	1556.44	1530	...
Skeleton of fetus	159.28	115	...
Gall bladder wall	3.08	8	8
Stomach contents	69.41	230	250
Stomach wall	81.80	140	140
SI contents	387.19	375	400
SI wall	322.81	600	600
Upper Large intestine contents	453.05	210	220
Upper Large intestine wall	281.43	200	200
Lower Large intestine contents	184.01	160	160
Lower Large intestine wall	118.74	135	135
Kidneys	529.41	275	275
Liver	2663.19	1400	1400
Ovaries	15.32	11	11
Pancreas	130.88	85	85
Placenta	628.33	310	462
Spleen	281.79	150	150
Urinary bladder contents	161.68	107	150-250
Urinary bladder wall	55.38	34.5	45
Uterus	1567.68	834	950
Whole body	91,000	61,500	58,000

To match organ masses in a tomographic model with those for the Reference Man is difficult even if the images are taken from a human subject that has identical height and weight as the

Reference Man. With the voxel-based geometry, one can artificially adjust the volume of an organ by reducing or increasing the number of voxels in a “trial and error” manner. This may be easier for organs such as the lungs that are large and round. On the other hand, organs such as skin and skeleton will not be as easy without losing the realistic nature of the images. Because organs and the total body are interlinked, manual adjustment at the voxel level can be time consuming if not impossible.

The supine position of a human subject during the procedures to obtain whole body images is not representative of a standing worker. The dosimetric effect of a reduced lung volume (see Table 1) in the supine position for the deceased subject is unknown. The tomographic models are generally more realistic than the stylized models. However, the image segmentation is extremely difficult and most of the models took months or years to be ready. A close examination of the organ boundary in the tomographic models reveals that the surfaces are no longer smooth due to the use of voxels. Fig. 3 illustrates this effect by comparing the images of thyroid glands displayed at three resolutions: 0.33mm, 1mm, and 4mm. As the voxel size increases, the organ surface becomes unacceptably distorted. This distortion can lead to remarkable dose uncertainty for low energy and less penetrating particles.

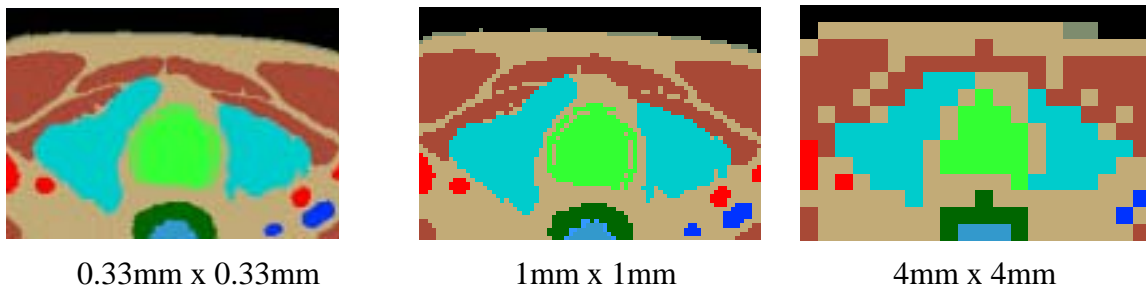


Fig. 3. Segmented VIP-Man images showing thyroid glands in blue in different pixel resolutions.

### 3.2 Effective Dose for The Adult Male

Effective doses for the stylized model were taken from ICRP 74/ICRU 57 [17, 20, 21]. Since photon exposures are the most common, this comparison provides an overall understanding of the most operationally relevant dosimetric discrepancies between these two types of anatomical models.

For the majority of the absorbed organ doses from the scaled VIP-Man model, the statistical errors are less than 3%. The statistical errors for effective dose, as propagated from each of the organ doses, are less than 1% practically in all cases. Therefore, the overall statistical precision of the reported results is very satisfactory, considering the extremely time-consuming calculations performed.

Figure 4 plots ratio of effective doses (stylized model divided by the scaled VIP-Man model) for photon beams incident on the body from various directions for energies from 20 keV to 10 MeV. For photon energies greater than 1 MeV, EDs differ by less than 10%, and for photon

energies between 60 keV and 1 MeV, the ED ratios are bound between 0.9 and 1.2 (i.e., maximum difference of 20%). These results show that the ED is not very dependent on the anatomical difference for the majority of the penetrating photon beams. Apparently the penetrating photons irradiate the body uniformly and doses from these two models at the organ level do not vary significantly. These results agree very well with Jones [22], Zankl et al. [23] and Kramer et al [24] who reported that the differences on ED between two types of anatomical models range from 20% to 38% for photon beam energies above 30 keV. However, for photon energies less than 30 keV, the ED ratio deviates from unity as the photon beams become less penetrating. For example, at 20 keV, the stylized model gives smaller EDs that are about 60%-80% of those from the scaled VIP-Man model for all directions, except for the PA direction where the ED from the stylized model is 180% of that from the scaled VIP-Man model. For photon energies nearing 10 MeV, the EDs from the stylized model are higher than those from the scaled VIP-Man model because “kerma approximation” was used in the work by Zankl et al while the EDs for the scaled VIP-Man were derived from EGS4 tracking secondary particles in photon interactions [21].

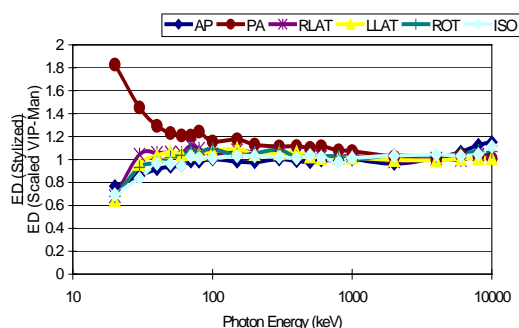


Figure 4. Comparison of effective doses (stylized model divided by the scaled VIP-Man model) for photon beams

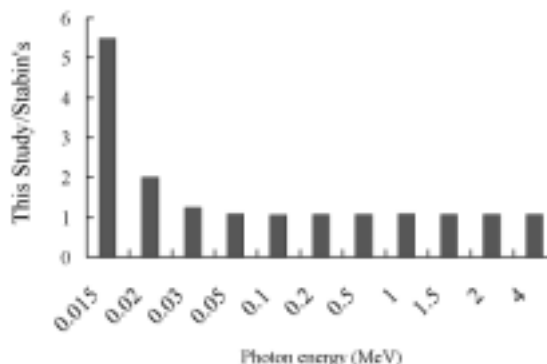


Figure 5. Comparison of SAFs for photons between the developed model and the 6-month mathematical model, where target is fetus and source is uterus

### 3.3 SAFs for Pregnant Woman Model

For the pregnant woman model, Figure 5 shows the ratios of SAFs for photons calculated from the tomographic model [11,12] to that of the stylized model developed by Stabin et al [15]. The target is the fetus and photons are located in the uterus. The results show that, although the organ locations and masses are different, the SAFs are practically the same for photons of energies greater than 50 keV. The difference is in the low energies as expected.

## 3. DISCUSSION AND CONCLUSION

Uncharged particles such as photons and neutrons (not presented here) are relatively penetrating. At the entire organ level, variations in anatomy do not change the doses very much. ED is a limiting quantity that is calculated as the weighted average of organ doses, and

is still less dependent on the anatomy for uniform external photon and neutron beams. Results shown in this study suggest that the EDs differ only by percentages that are insignificant, considering the uncertainties in the use of radiation and tissue weighting factors in the calculation of ED. In operational personnel dosimetry, uncertainties in dose measurement of up to 50% are not uncommon as a result of dosimeter energy calibration, positioning, environmental noise etc. It seems that a 20% change in the estimate of ED by the use of tomographic model may not justify the investment on the research in the past 15 years. In fact, if the same amount of resources were invested in refining the stylized models, one might have achieved the same degree of improvement on dose estimates for the photons and neutrons. The advantages of the stylized models include the following: 1) the stylized models described by surface equations (or similar mathematical means) are easy to standardize and to document; 2) stylized models are easy to implement in codes such as MCNP and EGS requiring minimum amount of computer memory; 3) Monte Carlo calculations are much faster because the number of boundaries is much less in the stylized models; 4) A lot of radiation protection data have already been accepted by different constituents such as the United States Nuclear Regulatory Agency, thus maintaining the necessary consistency.

The use of a tomographic model as a standard many cause new problems. First, it is very hard to identify one image set that resembles the Reference Man at both the torso and organ levels. Second, any image set would have certain imaging artifacts (such as the supine position during imaging) that are difficult or impossible to correct. Third, images must be segmented mostly by manual procedures that are painfully time consuming. Many internal organs cannot be reliably segmented from CT or MR images, leading to considerable human errors in the anatomical definition. Forth, for very small or thin organs and tissues, such as skin, eye lenses, the typical image pixel resolution of 2mm x 2 mm (many tomographic models have worse resolutions) is not good enough to represent the geometry truthfully. Lastly, the most important advantage of the tomographic models is their anatomical realism from the person-specific images. This advantage, ironically, is also the biggest drawback of the tomographic models because it is the long time wisdom of the community that no individual should be accepted as a reference man. One solution is to involve the creation of a family of such individuals so that, collectively, average values can emerge. However, by definition, any new addition to this family can change that average, which is a nightmare in setting standards and regulations.

Perhaps the best use of the tomographic models is to help refine the existing stylized models. Such refinement can reference the anatomical realism from the already developed tomographic models and additional medical data that are available to date. Voxel data can be combined with more complex surface equations, such as non-uniform rational b-splines (NURBS) to design hybrid models that define organ shapes more realistically than stylized models based on simple geometric primitives while maintaining the flexibility to consider anatomical variations and even body motion [25]. Such an ability to model a deformable object in 4D will be important in the next 5-10 years.

#### 4. REFERENCES

1. Snyder, W. S.; Ford, M. R.; Warner, G. G.; and Fisher H. L. Jr. Estimates of absorbed fractions for monoenergetic photon source uniformly distributed in various organs of a heterogeneous phantom. Medical Internal Radiation Dose Committee (MIRD) Pamphlet No.5, Supplement No. 3. Journal of Nuclear Medicine, 10. New York: Society of Nuclear Medicine, 1969.
2. Snyder, W. S.; Ford, M. R.; Warner, G. G.; and Fisher H. L. Jr. Estimates of absorbed fractions for monoenergetic photon source uniformly distributed in various organs of a heterogeneous phantom. Medical Internal Radiation Dose Committee (MIRD) Pamphlet No. 5, Revised. 1978.
3. M. Caon. Voxel-based computational models of real human anatomy: a review. Radiat Environ Biophys 42:229–235. 2004.
4. ICRP. 2002 Annual Report of the International Commission on Radiological Protection <http://www.icrp.org>.
5. ICRP. 2005 Draft Recommendations of the International Commission of Radiological Protection. [http://www.icrp.org/docs/2005\\_recs\\_CONSULTATION\\_Draft.pdf](http://www.icrp.org/docs/2005_recs_CONSULTATION_Draft.pdf)
6. Xu, X. G, Chao, T.C. Bozkurt A. Vip-Man: An Image-Based Whole-Body Adult Male Model Constructed From Color Photographs Of The Visible Human Project For Multi-Particle Monte Carlo Calculations. Health Phys. 78(5):476-486; 2000
7. Chao, T.C.; Xu, X. G. Specific Absorbed Fractions From The Image-Based Vip-Man Body Model And Egs4-VlSi Monte Carlo Code: Internal Electron Emitters. Phys. Med. Biol. 46: 901-927, 2001.
8. Chao, T.C.; Bozkurt, A.; Xu, X. G. Conversion Coefficients Based On Vip-Man Anatomical Model And Egs4-vlSi Code For Monoenergetic Photon Beams From 10 Kev To 10 Mev. Health Physics. 81(2):163-183, 2001.
9. Chao, T.C.; Bozkurt, A.; Xu, X. G. Organ Dose Conversion Coefficients For 0.1-10 Mev Electrons Calculated For The Vip-Man Tomographic Model. Health Physics. 81(2):203-214, 2001.
10. X. G. Xu And T. C. Chao. Calculations Of Specific Absorbed Fractions Of The Gi-Tract Using A Realistic Whole Body Tomographic Model. Cancer Biotherapy And Radiopharmaceuticals 18(3): 431-436, 2003.
11. Shi C.Y., Xu X.G. and Stabin M. G. Specific absorbed fractions calculated from a tomographic model of pregnant woman for internal photon emitters using Monte Carlo method. Health Physics. 87(5): 507-511. 2004.
12. Shi C.Y. and Xu X. G.. Development of a 30-week-pregnant female tomographic model from CT-images for Monte Carlo organ dose calculations. Medical Physics, Vol. 31(9):2491-2497. 2004.
13. Cristy, M. and Eckerman, K, Specific absorbed fractions of energy at various ages from internal photons sources, ORNL/TM-8381, V1-V7, Oak Ridge National Laboratory, Oak Ridge, TN, USA (1987).

14. ICRP. Report of the task group on Reference Man. ICRP Publication 23. Oxford: Pergamon Press, 1975.
15. M. G. Stabin, E. E. Weston, M. Cristy, J. C. Ryman, K. F. Eckerman, J. L. Davis, D. Marshall, and M. K. Gehlen, *Mathematical Models and Specific Absorbed Fractions of Photon Energy in the Nonpregnant Adult Female and at the End of Each Trimester of Pregnancy*, (Oak Ridge National Laboratory, Oak Ridge, TN, 1995), ORNL/TM-12907.
16. ICRP. Data for use in protection against external radiation. ICRP Publication 51. Oxford: Pergamon Press, 1987.
17. ICRP. Conversion coefficients for use in radiological protection against external radiation. ICRP Publication 74. Oxford: Pergamon Press, 1996.
18. Spitzer, V.M., and Whitlock, D.G. *Atlas of the Visible Human Male*. Jones and Bartlett Publishers, 1998.
19. ICRP. *Recommendations of the International Commission on Radiological Protection*. ICRP Publication 60. Oxford: Pergamon Press, 1991.
20. ICRU. Conversion coefficients for use in radiological protection against external radiation. ICRU Report 57. Bethesda, MD: International Commission on Radiation Units and Measurements, 1998.
21. Zankl M, Drexler G, Petoussi-Hens N and Saito K. The calculation of dose from external photon exposures using reference human phantoms and Monte Carlo methods: Part VII. Organ doses due to parallel and environmental exposure geometries GSF-Report 8/97 (München-Neuherberg: Institut für Strahlenschutz, GSF Forschungszentrum für Umwelt und Gesundheit) 1997.
22. Jones, D.G. A realistic anthropomorphic phantom for calculating organ doses arising from external photon irradiation. *Radiation Protection Dosimetry*. *Radiat. Prot. Dosim.* 77(1) (21-29), 1994.
23. Zankl M, Fill U, Petoussi-Hens N and Regulla D. Organ dose conversion coefficients for external photon irradiation of male and female voxel models *Phys. Med. Biol.* 47 2367–86. 2002.
24. R Kramer, J W Vieira, H J Khoury and F de Andrade Lima. MAX meets ADAM: a dosimetric comparison between a voxel-based and a mathematical model for external exposure to photons. *Phys. Med. Biol.* 49: 887–910. 2004.
25. X.G. Xu, and C. Shi. Preliminary Development Of A 4d Anatomical Model For Monte Carlo Simulations. Monte Carlo 2005 Topical Meeting. *The Monte Carlo Method: Versatility Unbounded In A Dynamic Computing World*”, Chattanooga, TN, April 17-21, 2005.